THERMO-ELECTRO-MECHANICAL MODELING OF A HALL-HÉROULT CELL COKE-BED PREHEATING

Daniel Richard[a], Patrice Goulet[b], Marc Dupuis[c], Jérôme Bédard[b] and Mario Fafard[b]

[a] Hatch, 5 Place Ville Marie, Bureau 200
Montréal, Québec, Canada, H3B 2G2

[b] Laval University, Science and Engineering Faculty,
Adrien-Pouliot Building, Sainte-Foy (Québec),
Canada, G1K 7P4

[c] GéniSim Inc., 3111 rue Alger,
Jonquière Québec, Canada, G7S 2M9

ABSTRACT

Start-up of a Hall-Héroult cell is a delicate task that can affect pot performance and pot life. Modern practices for high amperage cells involve preheating the lining before the molten electrolyte is poured in. Different preheating methods and heat-up schedules are used throughout the industry, and the optimum between a short start-up and damage minimization to the cell is elusive.

Direct electrical coke-bed preheating is one of the most common techniques. This practice typically results in a non-uniform surface temperature distribution and can generate detrimental thermal gradients in the cathode blocks. Numerical modeling is an invaluable tool to study this complex problem and can help improve the preheating procedures.

The modeling of the mechanical response of the lining is critical to detect risks of cathode block cracking or the development of gaps where liquids could leak into. Taking into account the baking of ramming paste, the quasi-brittle nature of carbon and the contact interfaces between different materials are examples of key elements to consider.

A finite element slice model of a cell was built and simulations of different electrical preheating scenarios were performed using the in-house code FESh++ to demonstrate what can be learned through thermo-chemo-mechanical modeling. The potential industrial application of the model is discussed.

INTRODUCTION

It is well accepted that start-up and early operation have a strong influence on the performance and life of a Hall-Héroult cell [1]. Generally, a preheating phase is necessary during start-up to ensure a smooth transition to normal operation.

As summarized in [2], some of the requirements for preheating are the following:

- The cathode block temperature must be high enough to:
  - Minimize bath freezing when bath is poured in. Freezing leads to an uneven current distribution and a potentially harmful unstable early operation.
  - Avoid large thermal gradients in the cathode blocks before bath is poured in. Large gradients may induce cracks.
- If the preheating rate is too fast or not uniform enough, large thermal gradients within the cathode blocks will occur and may also induce cracks.
- The paste temperature must be sufficiently high to avoid flash pyrolysis when bath is poured in.
- The lining must be maintained in compression at all times to ensure no gap is present in the lining as this would allow bath or metal penetration.

Complex phenomena are taking place during the start-up and early operation of a cell, for instance the transformations within the materials, the interaction of the lining with the pot shell and the electrical contact between the carbon electrodes and their metal conductors.

Direct electrical coke-bed preheating is one of the most common techniques. This practice typically results in a non-uniform surface temperature distribution and can generate large thermal gradients in the cathode blocks. To assess the risk of cell failure, the mechanical response of the cell must be studied.

Due to the intrinsic mechanical behaviour of the lining materials and the cell construction peculiarities, this is not a trivial task. Numerical modeling is therefore an interesting tool to help provide insights into these complex phenomena and help in designing the optimal procedure for a given cell.

As explained in some details in [2], the following aspects of the cell must be adequately taken into account to capture the key features of its mechanical behaviour.

Lining and potshell interaction

The response of the cell is *strain-driven*. Thermal expansion and chemical swelling generate elastic and potentially permanent deformation due to the confinement effect. The stress state of the lining therefore depends on the combined response of the cell components and the shell. The dilatometric and stress-strain behaviour of the cell materials must accordingly be known accurately.

Lining mechanical behaviour

The nature of several dense refractory materials, for instance the prebaked carbon cathode blocks, is very similar to that of concrete – they exhibit a *quasi-brittle* response. Some of their characteristics include the fact that their tensile strength is but a fraction of their compressive strength, that they can still bear some load after cracking and that their strength increases with confinement.

Material transformation and time-response

Preheating is intrinsically a transient problem. The response of the cell, for example the opening of gaps at the block-to-paste interface, will depend on the timing of several time-dependent phenomena. Ramming paste baking induces irreversible changes in its microstructure, which leads to macroscopic effects like swelling and subsequent contraction. The time-response of the paste to a sustained load (also known as creep) also depends on its baking state: it is obviously much more plastic when green.

Cell construction

Most of the cell components are laid without a strong bond between them. As in a masonry structure, joint behaviour has a profound effect on the stiffness and the response of the system. Contact interfaces must therefore be modeled to identify potential gap openings.

Also, for cell electrodes rodded using cast iron, the cast iron-to-carbon interface is critical. As shown in [3], contact may not occur everywhere, the contact resistance is pressure and temperature dependent, such that the thermal, electrical and mechanical responses are coupled primarily through Joule heating and thermal expansion.

FINITE ELEMENT DEMONSTRATION MODEL

For demonstration purposes, the same cell slice configuration used in [2] of a realistic prebaked point-fed 300 kA cell design inspired from a VAW publication [4] was used. The thermo-electrical results, using ANSYS, are presented in [5] for normal steady-state operation.

The slice mesh represents a quarter cathode and its corresponding lining, shell and cradle. The shell and cradle are discretized using large rotation shell elements while the lining is discretized using 3D brick elements. Half an anode was added to the original slice, as shown in Figure 1.

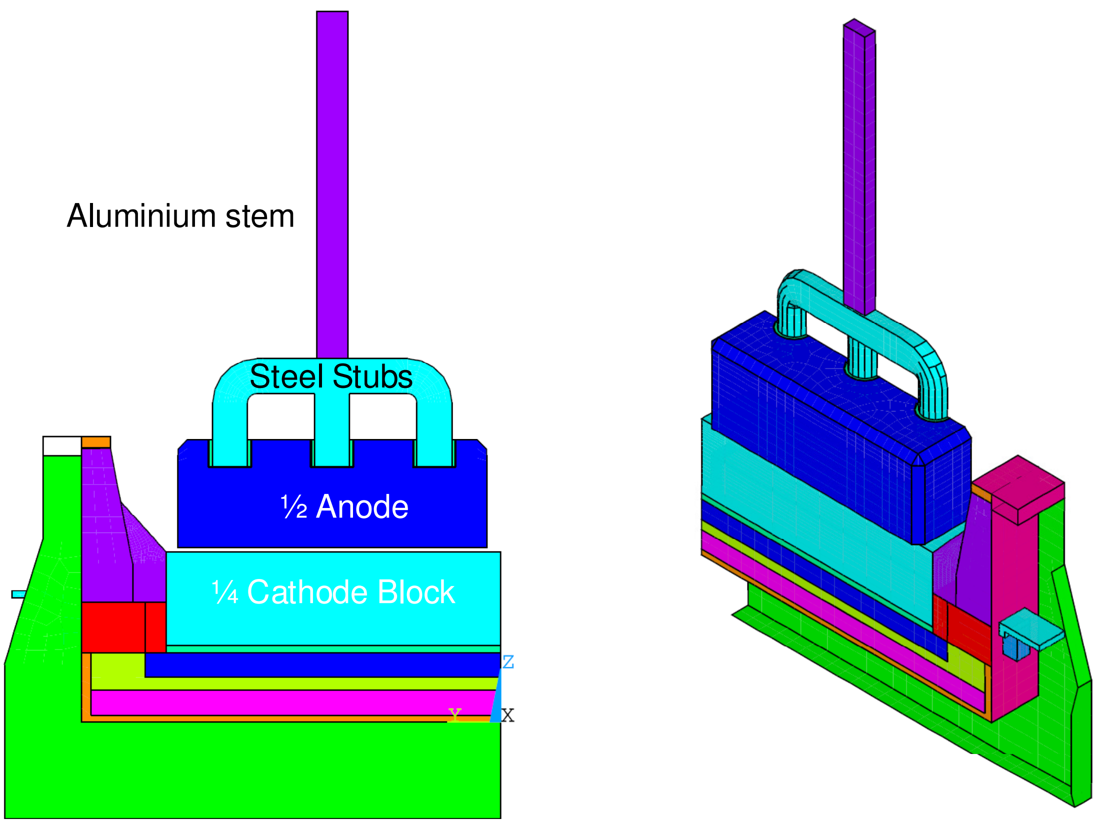

a) Side view

b) Isometric view

Figure 1 Cell Slice Finite Element Geometry

The mechanical behaviour of the anode assembly is nevertheless neglected and the anode contributes only to the thermal and electrical fields. The bottom surface of the anode is in contact with the top surface of the cathode block.

For this cell technology, the number of anodes does not match the number of cathodes such that half an anode carries more current than a quarter cathode block. Therefore, a “dummy” thermo-electrical slice is provided to ensure the correct amount of heat and current are flowing through the cathode block. This concept is shown in Figure 2a). Details of the lining are shown in Figure 2b).

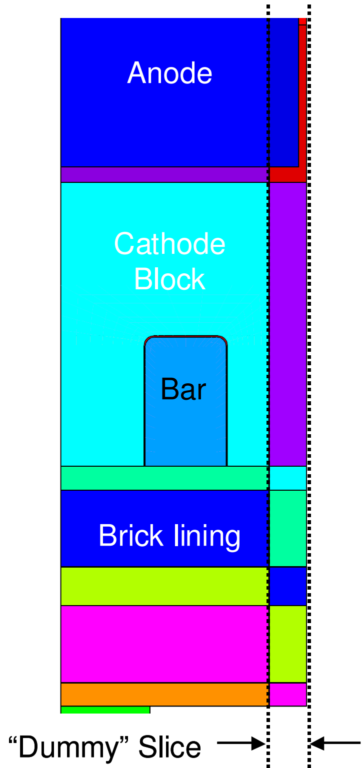

a) Dummy Slice Concept

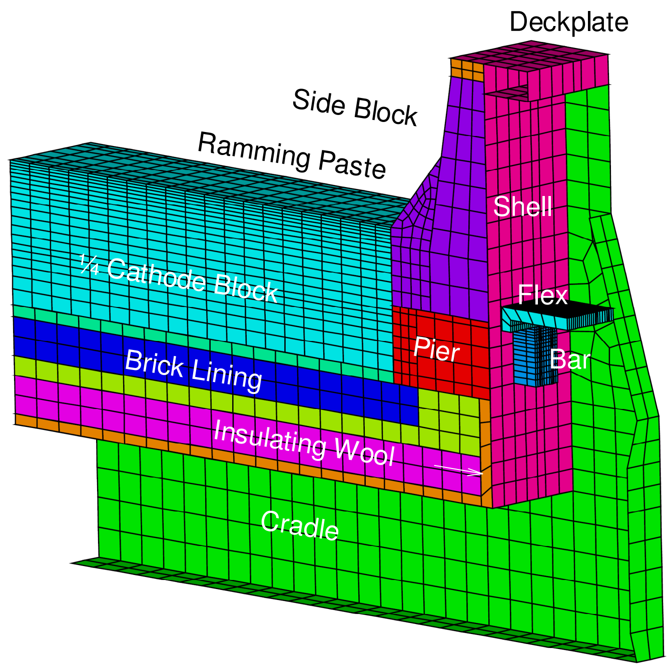

b) Cathodic Slice Finite Element Mesh

Figure 2 Cell Slice Model Details.

Contact mechanics is used between different parts of the lining, as can be seen from the non-concordant mesh at the interfaces between different parts in Figure 2b). An additional thermal contact resistance (constant or contact pressure-dependent) can be used at an interface, for example to emulate the effect of a mortar joint. Thermal conductance values were estimated from [10]. The interfaces are assumed to be non-cohesive, i.e. they cannot sustain a tensile stress. This is a conservative assumption, given that mortar is used in some places.

The cradles are welded to the shell, and the steel plate thicknesses were estimated from experience [11]. The collector bar is rodded with cast iron, and a simple geometry was assumed, as shown in Figure 3a). At ambient temperature, an air gap is present between cast iron and carbon, and as the assembly heats up, thermal expansion of the parts eliminates this air gap.

The brick lining under the cathode block is assumed to have no bending stiffness because in this design there is a layer of insulating refractory fiber wool that will absorb its thermal expansion in the horizontal plane. Therefore, the brick lining under the cathode does not contribute significantly to the mechanical response of the cell during preheating and is accordingly not solved in the mechanical problem. Conceptually, the cathode block and the pier are assumed to rest on springs of equivalent stiffness to the underlying brick lining. This is implemented in the finite element model by using contact mechanics to connect the shell floor to the bottom of the collector bar, of the cathode block and of the pier. The mechanical mesh is shown in Figure 3b). Note that the whole slice is solved for temperature (Figure 1).

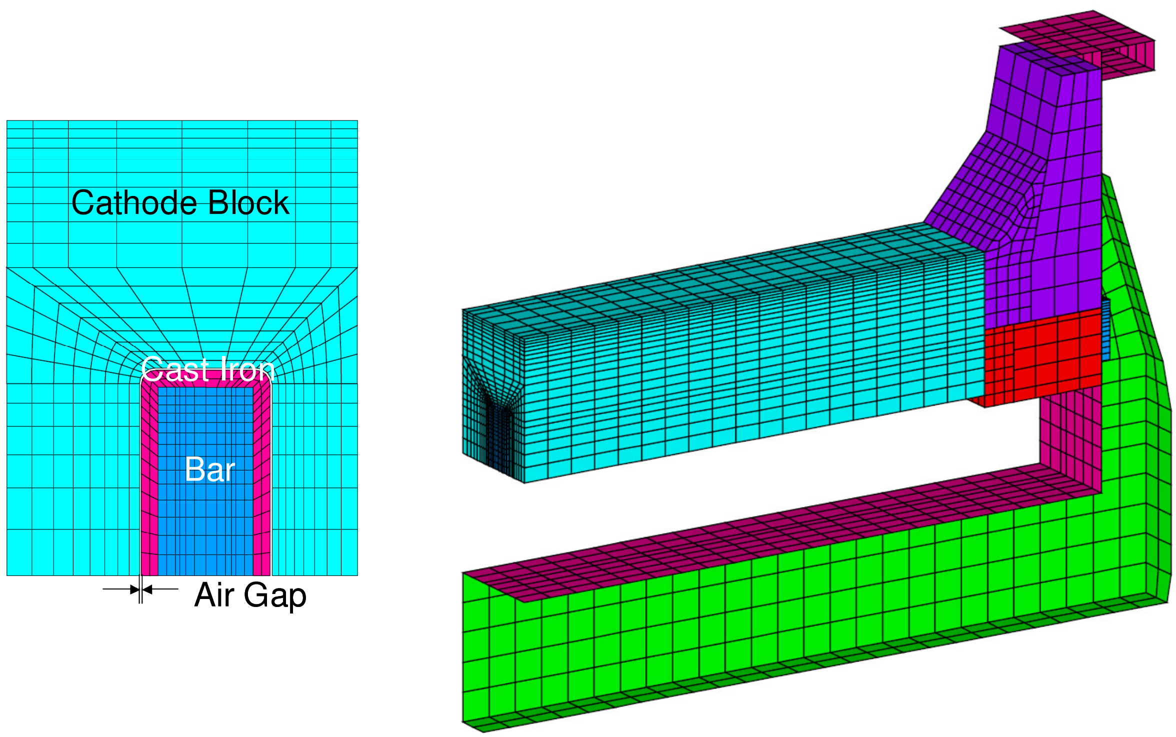

a) Cathode block assembly b) Mechanical slice mesh

Figure 3 Mechanical Slice Model Details.

<u>Material Properties</u>

The contact resistance at the anode/cathode block interface represents the effect of a 1-inch coke bed layer of uniform thickness. The effective resistance of the coke bed is temperature-dependent and inspired from [6]. Potential combustion of the bed is neglected.

The electrical contact resistance at the cast iron-to-cathode block interface is both pressure- and temperature-dependent is inspired from [12], as shown in Figure 4. A large resistance is used when physical contact is not achieved. All other thermal and electrical properties were taken from [5].

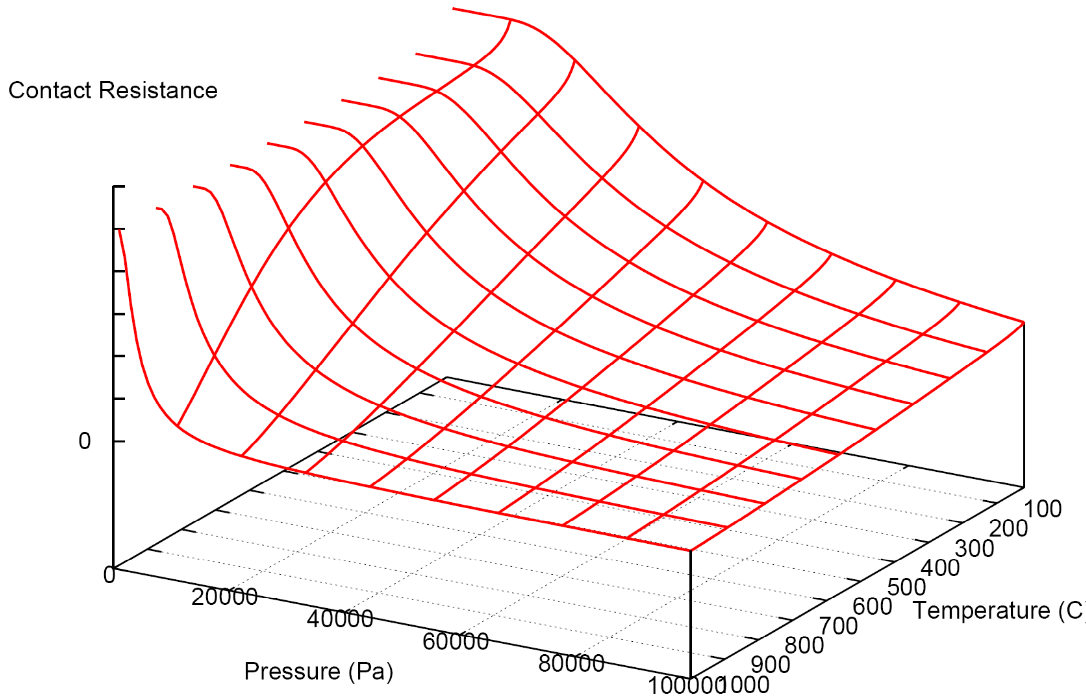

Figure 4 Electrical Contact Resistance at the Cast Iron to Cathode Block Interface.

The assumed mechanical constitutive laws are summarized in Table 1.

Table 1 - Assumed mechanical material models.

Material	Material Model	Reference
Cathode Block, semi-graphitic (30%)	Quasi-Brittle	[7]
Collector Bar	Elastic	[9]
Cast Iron	Elastic	[9]
Pier	Elastic	[9]
Ramming Paste	Reactive Quasi-Brittle	[8]
Side Block	Quasi-Brittle	[7]
Castable	Quasi-Brittle	[7]

Boundary Conditions and Loads

Since most of lining is free to move in the vertical upward direction, gravity must be included to stabilize the problem. This is the only external mechanical load considered.

The dashed lines in Figure 5a) represent planes S1, S2 and P3 on which symmetry conditions could be applied. Planes S1 and S2 are true symmetry planes, and P3 could be considered as such for the shell and cradle. However, the conditions on the latter are difficult to assess for the lining: they will depend on the interaction of the lining and the shell along the length of the cell, and will change with time. It was shown in [2] that the mechanical response of the cathode blocks changes significantly with the conditions on plane P3, to the extent that it was concluded that a slice model couldn't be used to predict the stress state of the lining during preheating. However, for this study and for comparison purposes only, the two extreme cases were nevertheless considered for the lining on plane P3: symmetry conditions, and free to move.

The thermal boundary conditions for all external surfaces take into account natural convection and grey body radiation, using well-known semi-empirical correlations and were taken from [5]. They are shown in Figure 5b). The surface of the ramming paste, of the anodes and of the sidewall is insulated by crushed bath and a convection coefficient of 1 W/m^2K was used to approximate this.

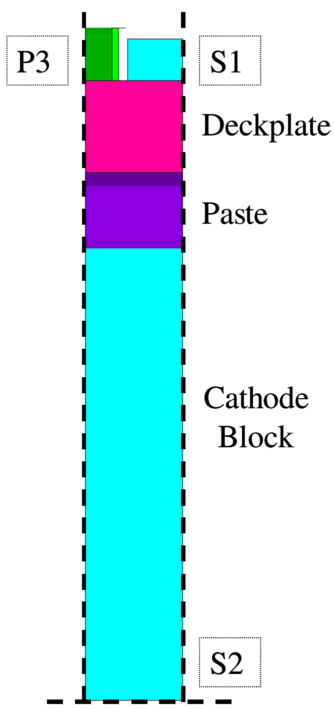

a) Slice symmetry planes, top view

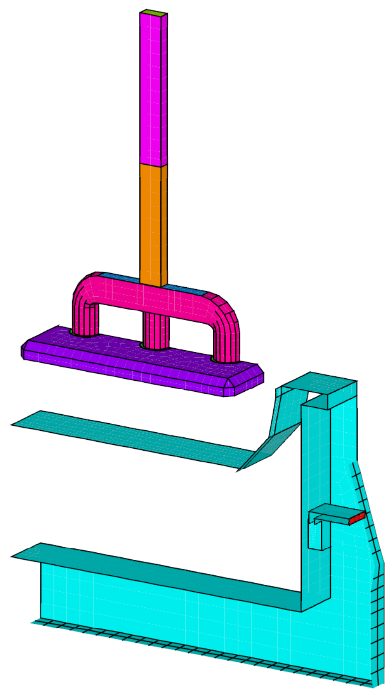

b) Convection surfaces

Figure 5 Boundary Conditions.

The anode stem to anode beam contact location is used as the electrical equipotential, and the current corresponding to a quarter cathode block is forced at the end of the flexible. The difference in current between the half-anode and the quarter-block is forced on the "dummy" cathode block to ensure the correct amount of current flows into the anode and the cathode parts.

A full line load preheating is compared to an arbitrary scenario involving the use of shunts, as shown in Table 2. A preheating time of 48 hours was chosen for the comparison basis to ensure a sufficient cathode surface temperature is achieved.

Table 2 - Shunt Removal Schedule.

Time	Number of Shunts	Fraction of current into cell
0 – 5h	4	60%
5 – 10h	3	70%
10 – 15h	2	80%
15 – 20h	1	90%
20 – 48h	0	100%

RESULTS AND DISCUSSION

Thermal

The thermal and electrical results are not significantly affected by the mechanical boundary conditions on plane P3 (Figure 5a). For the full line load case, the initial power input is very large compared to the case with shunts, as can be seen from the anode beam-to-cathode flex voltage drop in Figure 6. The total energy input to the cell is also larger in the full line load case.

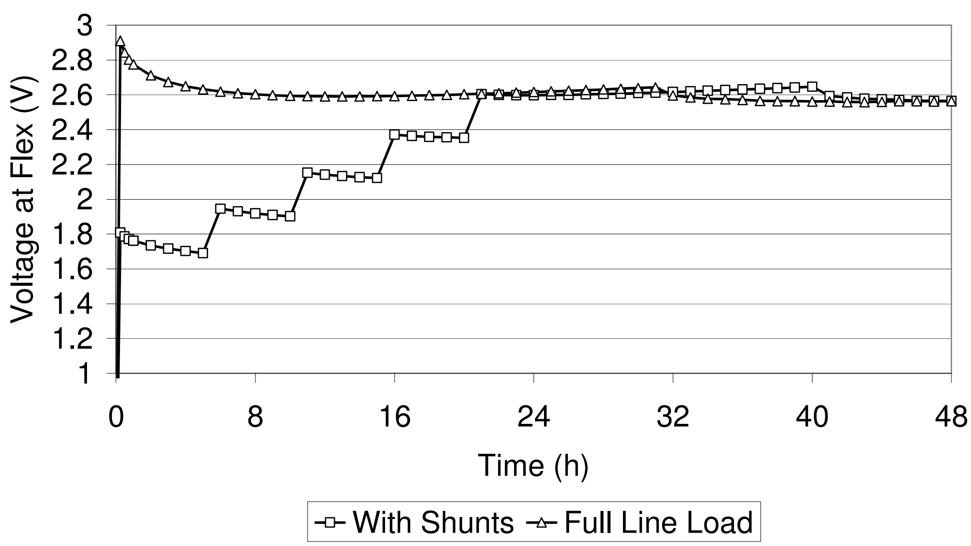

Figure 6 Anode Beam to Cathode Flex Voltage Drop.

Consequently, the temperature evolution is very different for full line load and with shunts. Figure 7 compares the maximum cathode surface temperature. It can be seen that the temperature rises very rapidly for the full line load case, and that the final surface cathode temperature is also larger in that case. The calculated corresponding heat up rate is compared in Figure 8. It can be seen that using shunts is an efficient way to control the heat up in the early stages of preheating, although there is a surge in power every time a shunt is removed.

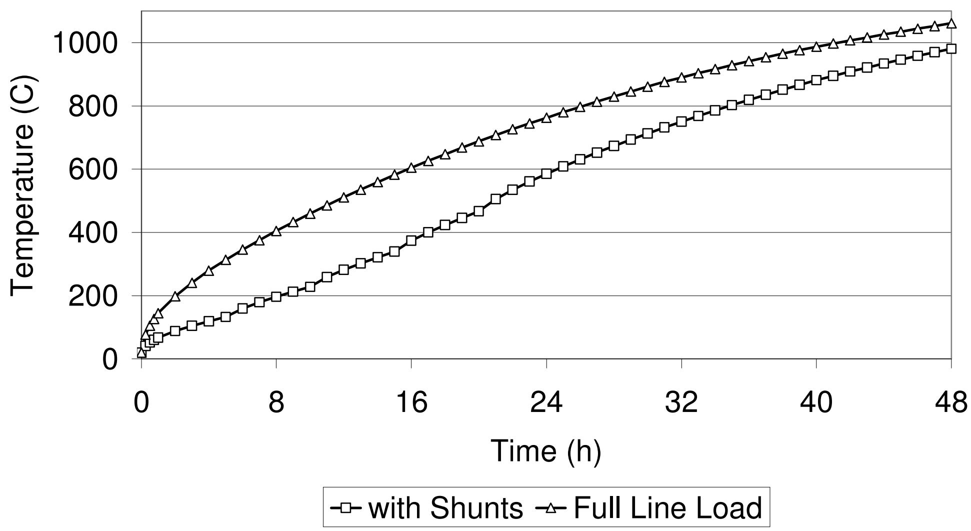

Figure 7 Evolution of Maximum Cathode Surface Temperature.

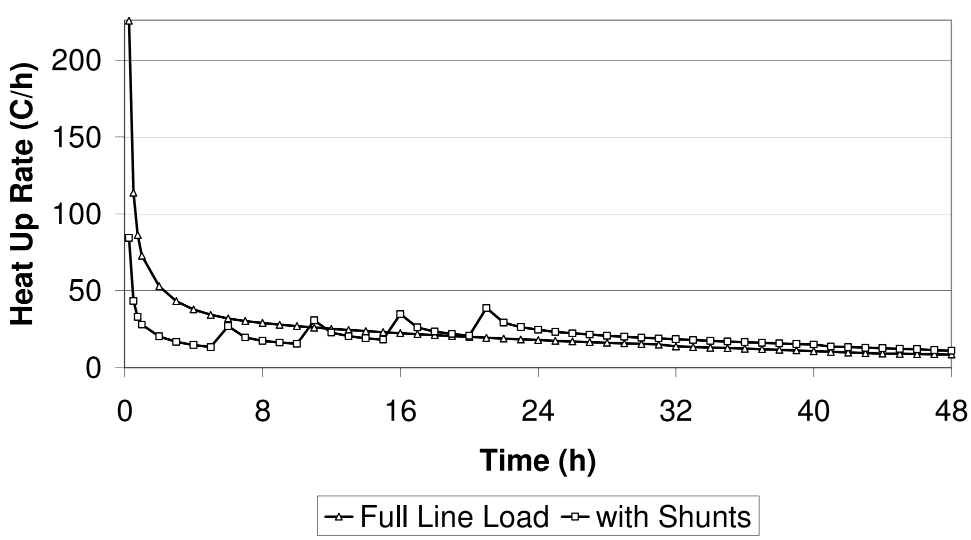

Figure 8 Calculated Heat up Rate at Maximum Surface Temperature Location.

As expected, the larger initial power input of the full line load case generates significant thermal gradients through the cathode block, as seen from Figure 9. The vertical gradients through the center of the block are significant, as shown in Figure 10; they will generate upward bending of the block, which has an effect on the electrical solution for the modeled configuration, as will be seen later.

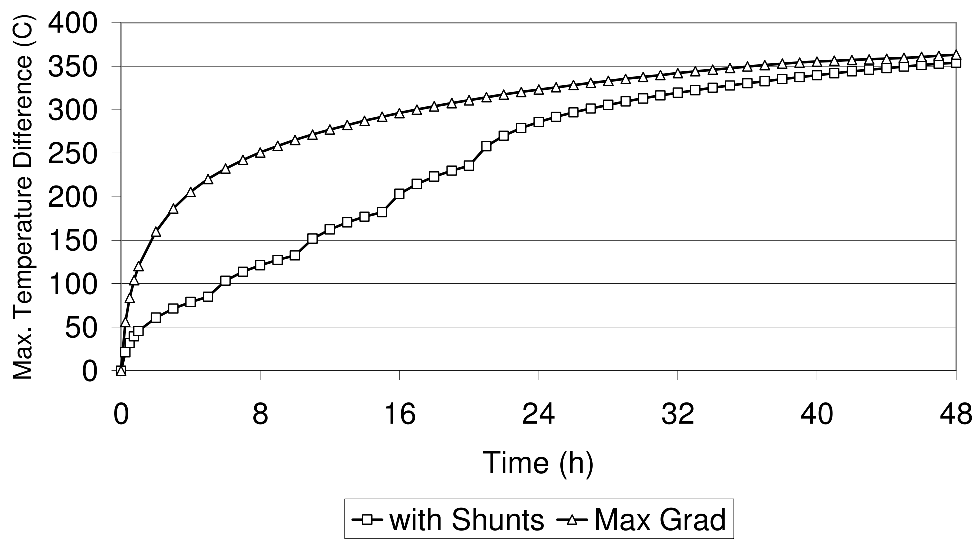

Figure 9 Evolution of Maximum Temperature Difference in Cathode Block.

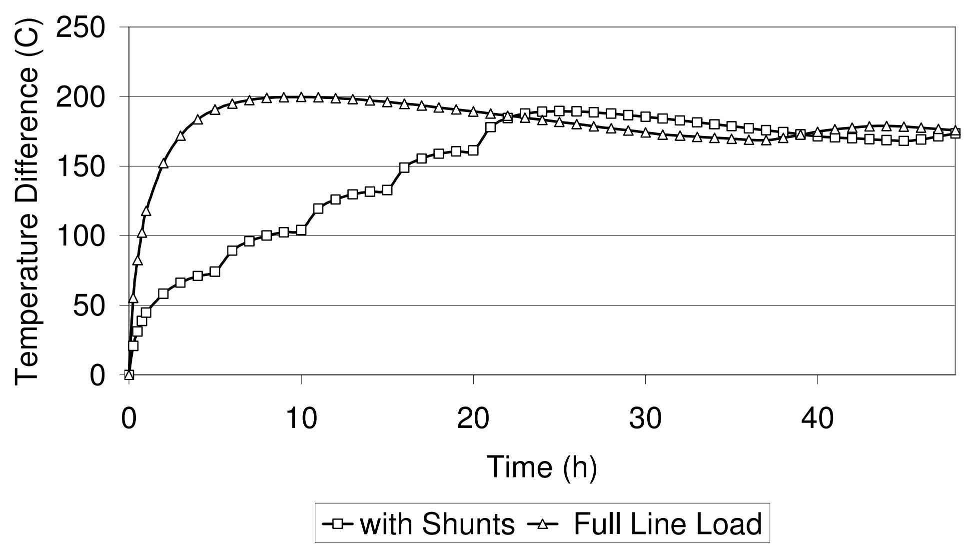

Figure 10 Evolution of Surface and Sub-cathodic Temperature Difference.

The final temperature distribution for both cases is shown in Figure 11 on the deformed lining. Note that the displacements are exaggerated for clarity. It can be seen that for the case with shunts, most of the cathode block surface temperature is below typical start-up bath freezing point while this is the case only at the end of the blocks for the full line load scenario.

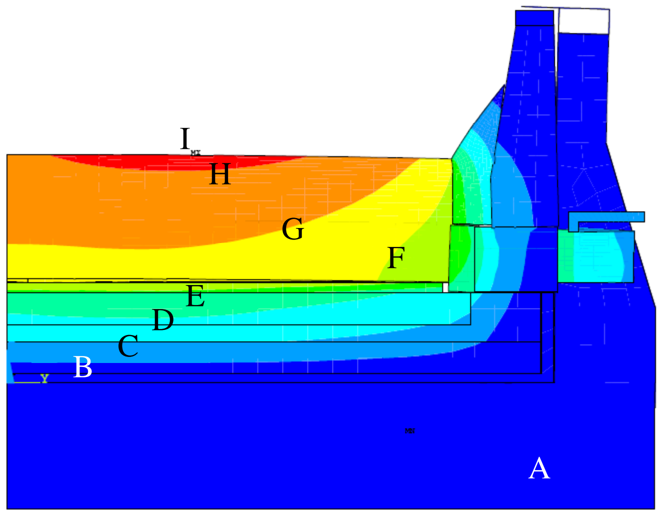

a) with Shunts

A:20 **B**:136 **C**:252 **D**:369 **E**:485 **F**:601 **G**:717 **H**:834 **I**:949 (ºC)

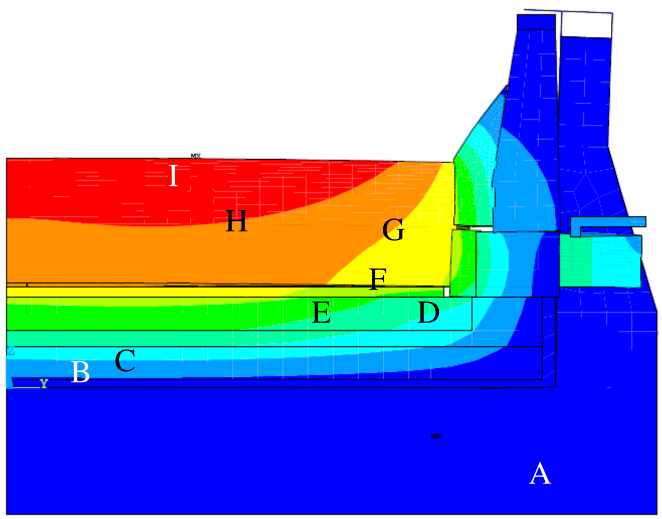

b) Full Line Load

Figure 11 Temperature Distribution after 48 hours.

An interesting effect of the transient diffusion of heat into the lining is that the extent of baking of the ramming paste changes with the use of shunts, as shown in Figure 12. Note that the local baking index is defined as the paste local compressive strength normalized to its strength at full baking (refer to [13] for more details). With the full line load case, the paste in the line of action of the cathode block is more rigid and less plastic than with the use of shunts, and its ductility is less. This allows a larger pressure to build up at the paste to cathode block interface, but will also reduce the ability of the paste to accommodate the expansion of the cathode block when bath will be poured in the cell. Given that paste also shrinks when it starts to bake, the timing of this process must be such that no gap will open where bath could leak into the lining.

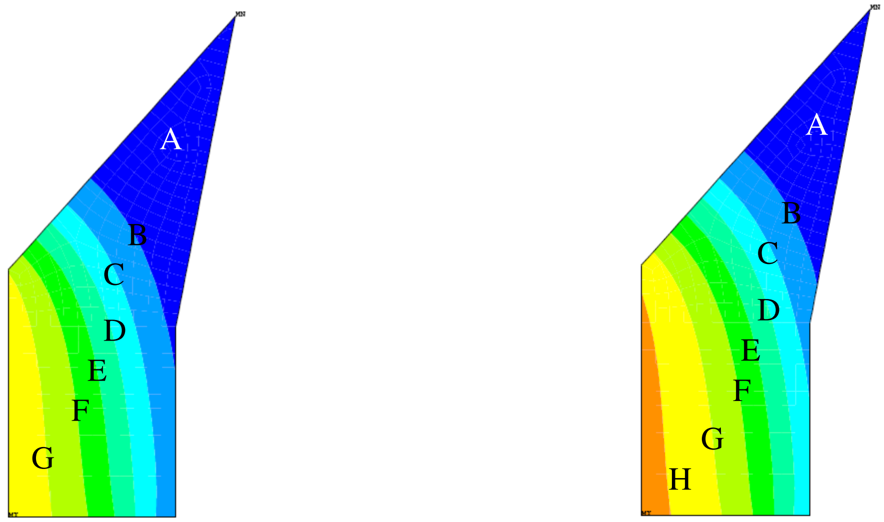

a) with Shunts b) Full Line Load

A: Green **B**:13 **C**:24 **D**:35 **E**:45 **F**:56 **G**:67 **H**:78 **I**:89 (%)

Figure 12 Ramming paste baking index at the end of preheating

During preheating, the vertical temperature gradients cause the cathode blocks to bend upwards, as seen in Figure 11. With the simple cathode block slot geometry and the low friction between cast iron and carbon, the cathode bar cannot be prevented from sliding in its slot. Therefore, the contact zone where current can flow in the bar becomes limited, as seen in Figure 13. The resulting evolution of the collector bar current pickup is shown in Figure 14. It is interesting to note that these results are nevertheless qualitatively consistent with published data on measured collector bar current pickup (see for example [14], Figure 7).

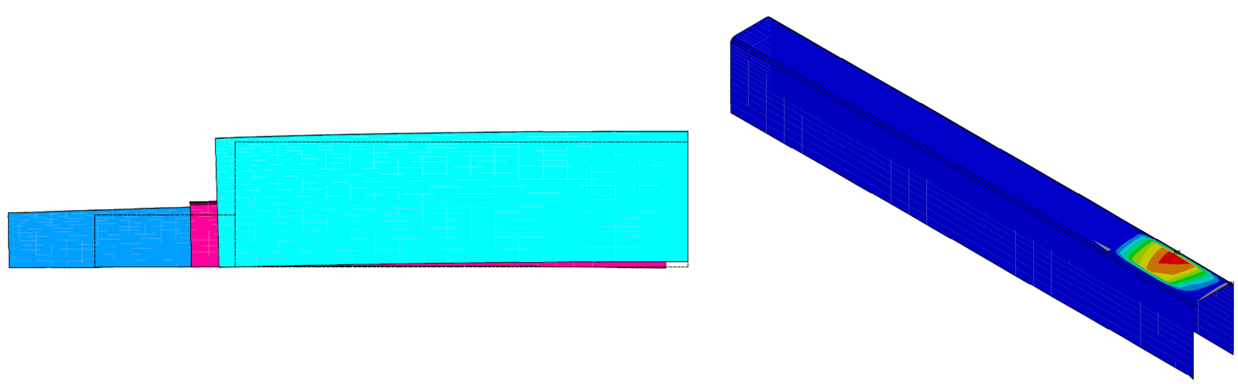

a) Exaggerated deformed shape b) Contact Pressure

Figure 13 Localisation of Cast Iron to Carbon Contact Zone after 48 hours, with Shunts.

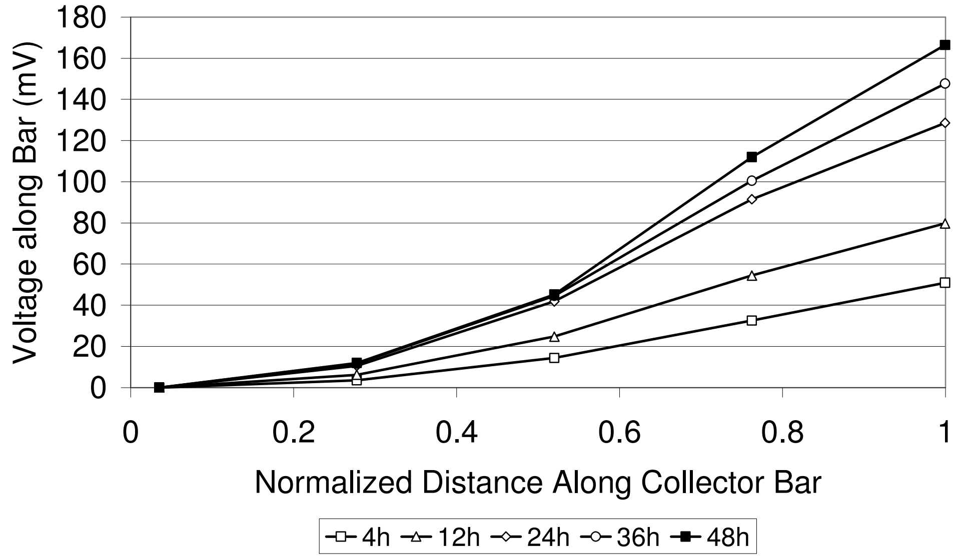

Figure 14 Collector Bar Current Pickup for Full Line Load Preheating.

<u>Mechanical</u>

The boundary conditions on the lining surface on plane P3 (Figure 5a) have a small impact on the overall displacements along the width of the cell, but have a large impact on the stress-strain behaviour of the lining. Two extreme cases were simulated: full symmetry and free to move. This corresponds respectively to an infinitely rigid shell, and to a perfect expansion joint along the length of the pot.

As expected, the cathode blocks are bending up and compress the ramming paste. Regarding potential opening of gaps in the lining, as the cathode block pushes up the paste, a gap opens between the ramming paste and the pier while the thermally induced deformation of the shell opens up a gap between the side block and the sidewall near the deckplate (Figure 11). This is similar to the results previously obtained for thermal bake-out [2].

It was found that the stress distribution in the lining was radically different for the two conditions on plane P3. For example, the first principal tensile stress is compared in Figure 15 for the case with shunts and after 25 hours of preheating. This is the moment where the vertical temperature gradient in the center of the block is maximum for that case, as shown in Figure 10. Note that the center of the cell is on the right hand side of the cathode block, and the ramming paste seam is on the left hand side. It can be seen that preventing the transverse expansion of the cathode block induces a large tensile stress zone originating from the slot wings.

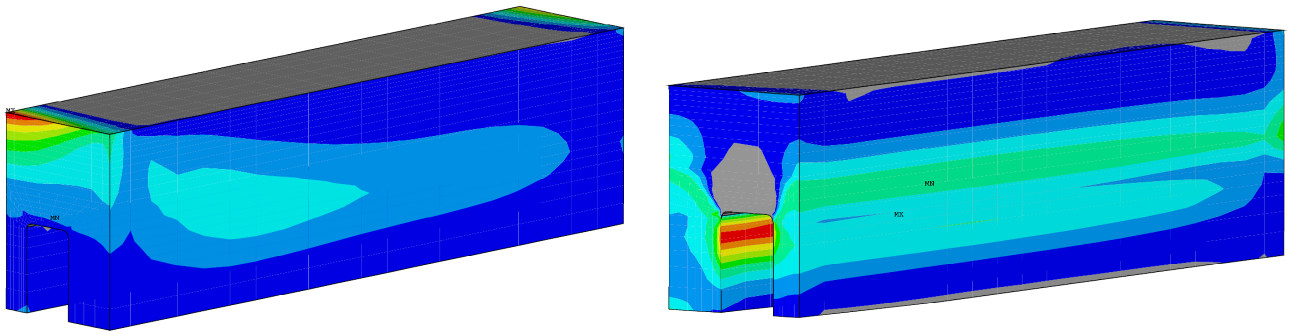

a) Plane P3 is free to move b) Plane P3 is a symmetry plane

Figure 15 First Principal Stress in the Cathode Block at 25h, with Shunts.

These tensile stresses are not sufficient to create permanent tensile deformation in the cathode block when plane P3 is free to move. However, when P3 is a symmetry plane, the fillet of the slots undergoes a localised permanent tensile strain, as shown in Figure 16a). Note that the block in the same orientation as in Figure 15 and that the grey zone is free of permanent strains.

This permanent tensile strain localisation is an indicator of potential cracking since the material is now beyond its yield stress. For the case with shunts, it has not reached its peak stress after 48 hours of preheating, but in the full line load case, cracking has occurred, as seen from the softening parameter shown in Figure 16b). This parameter represents the local equivalent permanent tensile strain beyond the peak stress of the material.

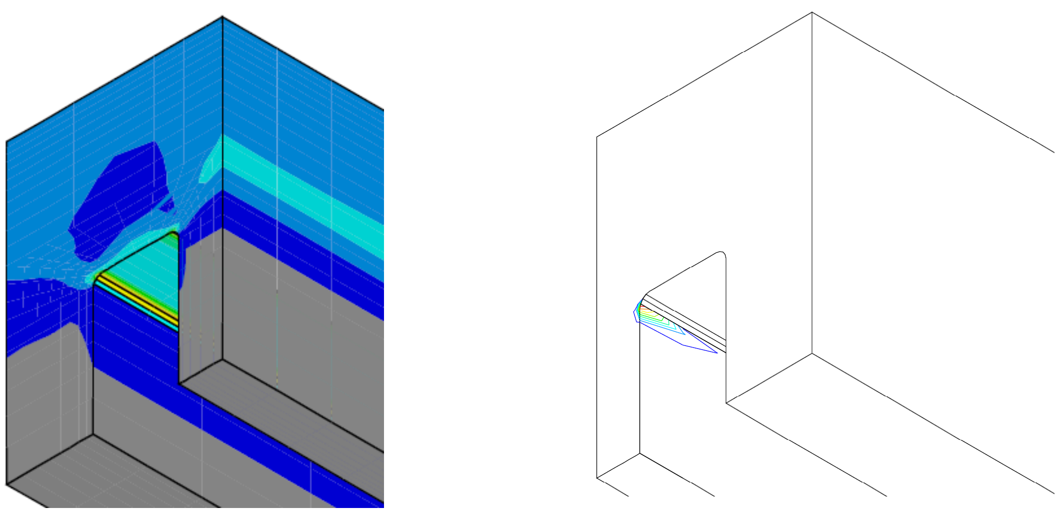

a) First Principal Permanent Tensile Strain in the Cathode Block Slot at 48h, with Shunts b) Softening Parameter in the Cathode Block Slot at 48 h, Full Line Load.

Figure 16 Cathode Block Cracking Indicators

CONCLUSION

The same conclusion than for the thermal bake-out simulation can be drawn [2]: although it had been previously demonstrated that a slice model might be used for the thermo-electric design of a cell [15], the significant difference of behaviour of the cathode block with the change in boundary conditions on plane P3 makes a slice model ill-suited to assess the mechanical behaviour during the preheating of a Hall-Héroult cell, unless the shell provided no confinement along the length of the pot, or otherwise if it were infinitely rigid. At least a quarter-cell must therefore be modeled to obtain a representative stress state in the lining.

However, these results strongly hint that some form of expansion relief must be provided along the length of the cell to prevent overstressing the cathode blocks.

Another interesting result from the model is that for our simple cathode block slot design, the relative displacement of the cathode block and the rodded bar during preheating causes a localised contact zone where current can flow into the bar. This is certainly far from the ideal, and a detailed study of cathode block-to-bar connection geometry would undoubtedly yield interesting findings

It can be argued that our arbitrary scenario involving the use of shunts is suboptimal, since the resulting heat-up rate as shown in Figure 8 is slightly increasing with time. In reality, the cell resistance should have been left to decrease further before removing the next shunt. Nevertheless, this illustrates how a numerical model can be used to help design better preheating procedures taking into account the coupled effects of thermal, electrical and mechanical phenomena.

Once validated on *in situ* measurements, the industrial application of such a model could also involve the development of control metrics. For instance, by relating appropriate results from the model – considered as the expected “theoretical results” – and the corresponding measurement on an actual cell, it may be possible to develop early warning signals and react accordingly.

ACKNOWLEDGEMENTS

The authors wish to thank Lowy Gunnewiek from Hatch for his support and for the useful discussions and comments. The kindness of Professor Daniel Marceau from Université du Québec à Chicoutimi is also acknowledged, for providing us with an access to his numerical computing facilities. Finally we thank the Natural Sciences and Engineering Research Council of Canada (NSERC) and REGAL for the granted partial financial assistance.

REFERENCES

[1] M. Sørlie & H.A. Øye, Cathodes in Aluminum Electrolysis, 2nd Edition, Aluminium-Verlag, 1994.

[2] D. Richard, P. Goulet, M. Dupuis & M. Fafard. "Thermo-Chemo-Mechanical Modeling of a Hall-Héroult Cell Thermal Bake-out', in Proceedings of TMS Light Metals 2006, p. 669-674

[3] Richard, D., Fafard, M., Lacroix, R., Cléry, P., Maltais, Y., 2001. "Aluminum reduction cell anode stub hole design using weakly coupled thermo-electro-mechanical finite element models", Finite Elements in Analysis and Design, **37** (4), 287–304

[4] V.A. Kryukovski, G.A. Sirasutdinov, J. Klein & G. Peychal - Heiling, "International Cooperation and High-Performance Reduction in Siberia", JOM, **46** (2), 1994, 23-25.

[5] M. Dupuis, "Thermo-Electric Design of a 400 kA Cell: A Tutorial", in Proceedings of TMS Light Metals 2000, 297-302.

[6] C. Laberge, L. Kiss & M. Désilets. "The Influence of the Thermo-Electrical Characteristics of the Coke-Bed on the Preheating of an Aluminium Reduction Cell", in Proceedings of TMS Light Metals 2004, p.207-211.

[7] G. D'Amours, M. Fafard, A. Gakwaya & A. Mirchi. "Multi-Axial Mechanical Behavior of the Carbon Cathode: Understanding, Modeling and Identification", in Proceedings of TMS Light Metals 2003, 633-639.

[8] D. Richard, G. D'Amours, M. Fafard, & M. Désilets. "Development and Validation of a Thermo-Chemo-Mechanical Model of the Baking of Ramming Paste", in Proceedings of TMS Light Metals 2005, 733-738.

[9] Y. Sun, K.G. Forslund, M. Sørlie & H.A. Øye, "Modelling of Thermal and Sodium Expansion in Prebaked Aluminium Reduction Cells", in Proceedings of TMS Light Metals 2004, 603-610.

[10] P. Goulet, “Modélisation du comportement thermo-électro-mécanique des interfaces de contact d’une cuve de Hall-Héroult”, Ph.D. Thesis, Laval University, November 2004, 289 pages.

[11] M. Dupuis & D. Richard, “Study of the Thermally-induced Shell Deformation of High Amperage Hall-Héroult Cells”, in Proceedings of COM 2005, 35-47

[12] Richard, D., Fafard, M., Lacroix, R., Cléry, P., Maltais, Y., 2003. “Carbon to cast iron electrical contact resistance constitutive model for finite element analysis”. Journal of Material Processing Technology, **132** (1–3), 119–131.

[13] D. Richard, G. D’Amours, M. Fafard, & M. Désilets. “*Development and Validation of a Thermo-Chemo-Mechanical Model of the Baking of Ramming Paste*”, in Proceedings of TMS Light Metals 2005, 733-738.

[14] R.F. Boivin, P. Desclaux & J.P.R. Huni, “Cathode Collector Bar Temperature and Current Pickup”, In Proceedings of TMS Light Metals 1985, p. 625-635.

[15] M. Dupuis, “Thermo-Electric Analysis of the Grande-Baie Aluminum Reduction Cell”, in Proceedings of TMS Light Metals 1994, p. 339-342.